SOLIDS FLOW CHARACTERISTICS IN LOOP-SEAL OF A CIRCULATING FLUIDIZED BED

Sung Won Kim, Won Namkung and Sang Done Kim[†]

Department of Chemical Engineering and Energy & Environment Research Center,
Korea Advanced Institute of Science and Technology, Taejon 305-701, Korea

Abstract – The hydrodynamics of solids (FCC) recycle in a loop-seal (0.08 m) at the bottom of the downcomer (0.08 m-I.D.×4.0 m-high) in a circulating fluidized bed (0.1 m-I.D.×5.3 m-high) have been determined. Solid flow rate through the loop-seal increases linearly with increasing aeration rate. At the same aeration rate, the maximum solid flow rate can be obtained at a loop-seal height-to-diameter ratio of 2.5. The effects of solid inventory, solid circulation rate and gas velocity on pressure balance around the CFB have been determined. At a given gas velocity and solid circulation rate, pressure drops across the downcomer and loop-seal increase linearly with increasing solids inventory in the bed. At a constant solid inventory, pressure drops across the riser and the downcomer increase with increasing solid circulation rate but decrease with increasing gas velocity in the riser. The obtained solid flow rate has been correlated with pressure drop across the loop-seal.

Key words: Circulating Fluidized Bed, Solid Recycle System, Loop-Seal, Non-Mechanical Valve, Downcomer

INTRODUCTION

Circulating fluidized beds (CFB) have been commercially used in numerous gas-solid contacting processes such as combustors and catalytic reactors because of the good gas-solid contact [Namkung et al., 1994; Cho et al., 1994]. In general, a CFB is composed of a riser, cyclone and solid recycle system, which consists of a downcomer, and a solid feeding system. Solid recycle systems provide solids transfer from lower to higher pressure points and gas seal against the undesirable flow direction, and regulate solid circulation rate [Rudolph et al., 1991].

The solid feeding devices are divided into mechanical and non-mechanical valves [Yang and Knowlton, 1993]. Typical mechanical valves having moving parts to control solid flow rate are rotary, screw, butterfly and slide valves. These valves cannot be easily employed under high temperature and pressure conditions due to sealing and mechanical problems. For applications of elevated temperature and pressure conditions, non-mechanical valves such as loop-seal, L-, J-, and V-valves are commonly employed. The non-mechanical valves without moving parts can control solid flow rate by aeration. It has been reported that the major problem in CFB operation is interruption of feeding or transferring of particulate solids [Merrow, 1985]. Therefore, the proper operation of a solid feeding system is crucially important for safe and stable operation of a CFB process. Various experimental studies on non-mechanical valves such as the L-valve [Yang and Knowlton, 1993; Knowlton and Hirsan, 1978; Geldart and Jones, 1991], J-valve [Knowlton and Hirsan, 1978], V-valve [Leung et al., 1987] have

been reported. However, studies on loop-seal systems are comparatively sparse in spite of wide application in commercial CFBs. Moreover, most of the studies on non-mechanical valves have been conducted in a separate solid recycle system rather than a system incorporating a riser.

In the present study, the solids recycle characteristics of a loop-seal have been determined in a CFB system, and the hydrodynamic behavior in a downcomer has been determined under various operating conditions. The solid circulation rate has been correlated with pressure drop across the loop-seal.

EXPERIMENTAL

Experiments were carried out in a solid recycle system incorporating a riser (0.1 m-I.D.×5.3 m high) as shown in Fig. 1. The solids recycle system is composed of a downcomer (0.08 m-I.D.×4.0 m high) and a loop-seal (0.08 m-I.D.) as a solid feeding device. The solid particles used in the present study were FCC particles and their properties are given in Table 1. The details of the experimental facilities can be found elsewhere [Namkung et al., 1994; Cho et al., 1994] except for the solid feeding system. The entrained particles from the riser were collected by the primary and secondary cyclones and stored in a hopper. The solid particles from a hopper were transferred into a loop-seal through a downcomer (0.08 m-I. D.), and it was fed to the riser through a loop seal with regulation of solids circulation rate (G_s) by aeration. The superficial gas velocity (U_g) and G_s were varied in the range 2.0-4.0 m/s and 0-27 kg/m²s, respectively. Also, solid inventory in the system was varied in the range 10-40 kg. Air was injected into the loop-seal at two locations as shown in Fig. 2. A pipe sparger was located at the bottom of the loop-seal for bottom aeration and the other one was located perpendicular

[†]To whom correspondence should be addressed.
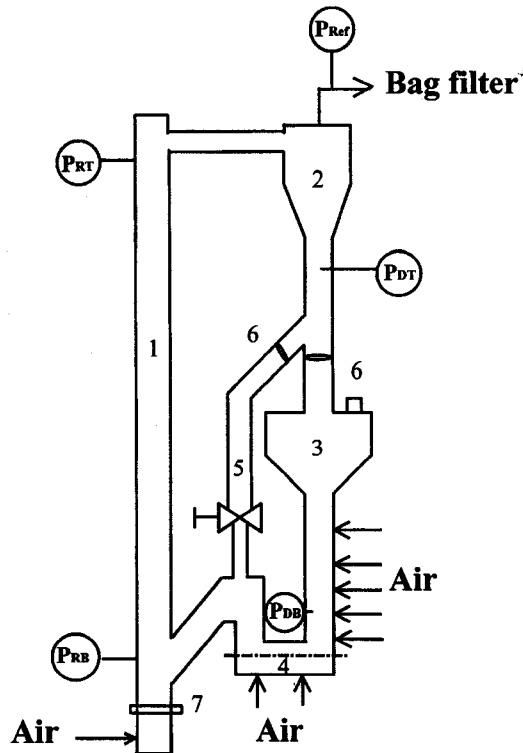E-mail: kimsd@cais.kaist.ac.kr

Fig. 1. Schematic diagram of apparatus.

1. Riser	5. Sampling pot
2. Cyclone	6. Butterfly valve
3. Hopper	7. Distributor
4. Loop-seal	

Table 1. Physical properties of FCC particle

	FCC particle
Mean diameter [μm]	65
ε_p	0.430
ε_{mf}	0.494
ϕ_s	0.625
Apparent density [kg/m^3]	1720
Terminal velocity [m/s]	0.19
Transport velocity [m/s]	1.40
U_{mf} [m/s]	0.0027

to the wall of the vertical section in the loop-seal for vertical aeration. For vertical aeration, air was injected at one of the different heights (0.1, 0.2, 0.4, 0.6 m) above the bottom of the loop-seal. Pressure taps were mounted flush with the walls of the riser, cyclone, downcomer and loop-seal to measure pressure drops around the CFB loop and connected to pressure transducers (Cole-Parmer T30, R42). A data acquisition system was used to record the instant pressure signals. The solid circulation rate around the CFB loop was measured by diverting the entire solids flow from the two cyclones into a sampling bottle. The descending solid circulation rate was determined by measuring the weight of solids through a known distance in a transparent sampling bottle with time.

DATA ANALYSIS

Variations of voidage in a downcomer are different types
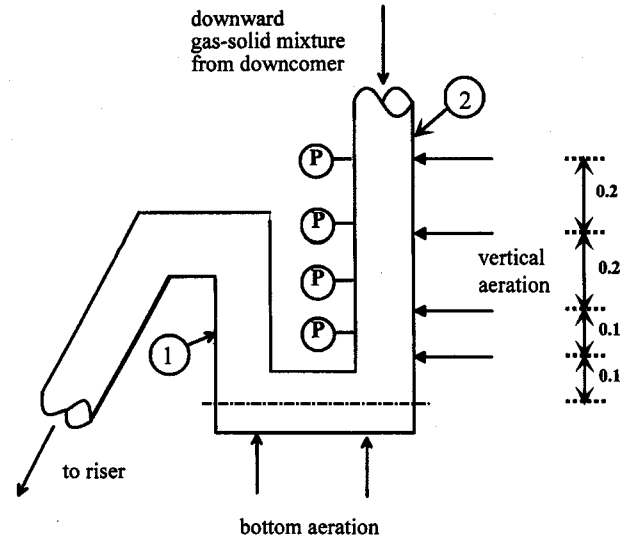

Fig. 2. Schematic diagram of loop-seal.
(1) Weir section, (2) Vertical aeration section.

with solid flow mode [Kojabashian, 1958]. In a fluidized bed flow or streaming flow in downcomer, voidage would be at the minimum fluidization condition (ε_{mf}) or above. Non-fluidized bed flow is divided into a packed bed (ε_p) and transitional packed bed flow. The transitional packed bed flow occurs when solids flow by aeration [Zhang and Rudolph, 1991]. Pressure drop in the solids flow by aeration can be expressed by the Ergun equation [Ergun, 1952] that is a function of slip-velocity (U_{sl}) as shown [Knowlton and Hirsan, 1978; Zhang and Rudolph, 1991].

$$\frac{dp}{dz} = \frac{150\,\mu(1-\varepsilon)^2 U_{sl}}{(\varphi_s d_p)^2 \varepsilon^2} + \frac{1.75\,\rho_s(1-\varepsilon)U_{sl}^2}{(\varphi_s d_p)\varepsilon} \qquad (1)$$

The slip velocity can be expressed as

$$U_{sl} = \frac{G_s}{\rho_s(1-\varepsilon)} - \frac{U_{gd}}{\varepsilon} = U_s - \frac{U_{gd}}{\varepsilon} \qquad (2)$$

When the Reynolds number is less than 20, the second term of Eq. (1) can be neglected so that Eq. (1) is simplified as Eq. (3) [Zhang and Rudolph, 1991].

$$\frac{dp}{dz} = K_l U_{sl}, \quad K_l = \frac{150\,\mu}{(\varphi_s d_p)^2}\left[\frac{(1-\varepsilon)}{\varepsilon}\right]^2 \qquad (3)$$

With the known values of solids circulation rate, gas velocity (U_{gd}) and the measured pressure drop in the downcomer, the bed voidage can be calculated from Eqs. (2) and (3). However, the measurement of U_{gd} is difficult so that another relationship between slip velocity and bed voidage is needed. Knowlton and Hirsan [1978] reported that variation of bed voidage in a transitional packed bed flow exhibits linearity with slip-velocity as Eq. (4) based on Kojabashian's classification [Kojabashian, 1958].

$$\varepsilon = \varepsilon_p + KU_{sl} \qquad (4)$$

Knowlton and Hirsan [1978] applied Eq. (4) to a standpipe with an L-valve, and Zhang and Rudolph [1991] applied it to

a standpipe with an orifice. Also, they proposed the following equation to predict the variation of bed voidage as

$$\varepsilon = \varepsilon_p + \frac{|U_{sl}|}{(U_{mf}/\varepsilon_{mf})}(\varepsilon_{mf} - \varepsilon_p) \qquad (5)$$

Therefore, in the present study, bed voidage and slip-velocity in the transitional packed bed flow are calculated by using the measured pressure drop in the downcomer by Eqs. (3) and (5).

RESULTS AND DISCUSSION

1. Pressure Balance

In a circulating fluidized bed, pressure in the loop should be balanced for stable operation. The pressure drop across the downcomer can be expressed as [Rhodes and Laussmann, 1992]

$$\Delta P_d = \Delta P_{ls} + \Delta P_r + \Delta P_c \qquad (6)$$

The effect of solid inventory on the pressure balance in the CFB loop is shown in Fig. 3. As can be seen, the effect of solids inventory at the given U_g and G_s on pressure drop across the riser is found to be small as reported by Rhodes and Laussmann [1992]. As expected, the pressure loss across the primary cyclone and pipe connecting to the top of the riser is unaffected by variation of solid inventory at the given U_g and G_s. Pressure drop across the downcomer increases linearly with increasing solids inventory. The solids flow in the downcomer is in the packed bed flow mode having a constant bed voidage by aeration at the loop-seal. Therefore, an increase in pressure drop across the downcomer is caused by air flow through the packed bed whose height increases in proportion to solid inventory. It can be also observed that the pressure drop across the loop-seal increases linearly with increasing pressure drop in the downcomer to maintain pressure balance.
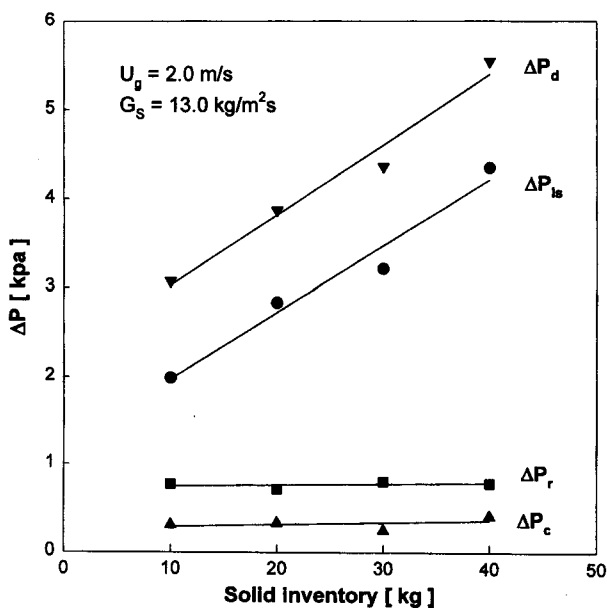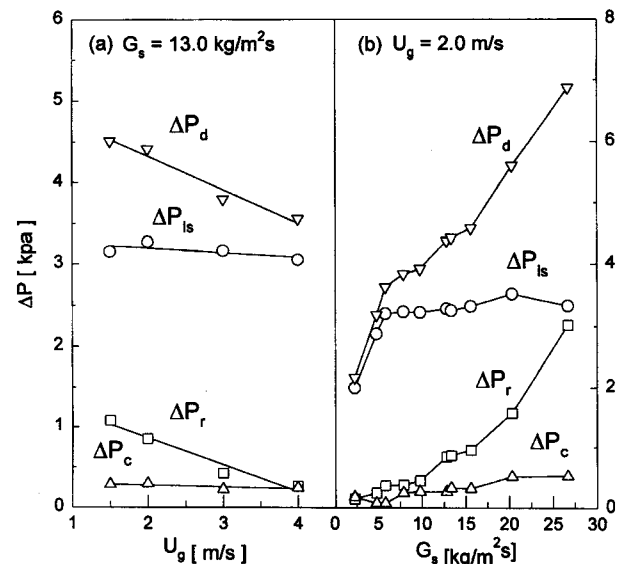

Fig. 4. (a) Effect of gas velocity on pressure balance in the CFB loop (I=30 kg ; G_s=13.0 kg/m²s), (b) Effect of solid circulation rate on pressure balance in the CFB loop (I= 30 kg ; U_g=2.0 m/s).

The effects of U_g and G_s on pressure balance in the CFB loop are shown in Fig. 4. As expected, pressure drop in the riser increases with increasing G_s at constant U_g and decreasing U_g at constant G_s due to increment of solid holdup. The pressure drops across the cyclone and the loop-seal are practically unaffected by U_g. However, the pressure drops across the cyclone and the loop-seal somewhat increase with increasing G_s due to the increase of pressure loss with increasing G_s [Rhodes and Laussmann, 1992]. The increase of pressure drop in the downcomer is matched by a similar increase in pressure drop in the riser for pressure balance in the CFB loop.

2. Characteristics of Loop-Seal

2-1. Components and Functions of Loop-Seal

A loop-seal consists of weir and vertical aeration sections (Fig. 2). When air is injected at the bottom and the vertical aeration sections in the loop-seal, solid particles begin to flow with fluidity and they are transferred from the vertical aeration section to the weir section. In the weir section, the transferred solid particles overflow into the riser. In the vertical aeration section, pressure builds up in the downcomer by aeration for solids flow in the CFB loop. In the weir section, solid particles in the loop-seal are transported into the riser with higher pressure than that in the bottom of the riser to provide gas flow in the riser direction [Basu and Fraser, 1991].

2-2. Solids Flow Characteristics by Bottom Aeration

The effect of bottom aeration velocity on solid circulation rate at a given vertical aeration rate (U_A=4U_{mf}) is shown in Fig. 5. As can be seen, solid particles do not flow by the vertical aeration only due to stagnation of packed solids in the weir section. However, air is injected at the bottom of the loop-seal, solid particles attain fluidity and are transported into the riser. Solids circulation rate through the loop-seal increases to a maximum value with increasing bottom aeration rates up to 1.5U_{mf}. However, bottom aeration rates above 1.5U_{mf} do not
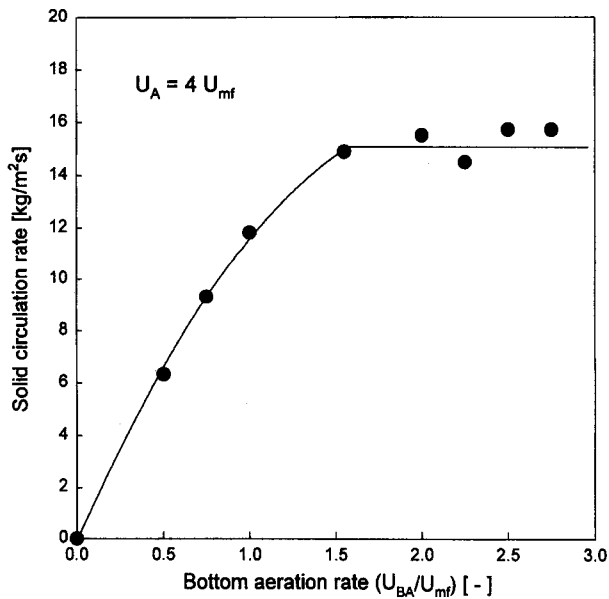

Fig. 3. Effect of solid inventory on the pressure balance in the CFB loop (U_g=2.0 m/s, G_s=13.0 kg/m²s).

Fig. 5. Effect of bottom aeration velocity on solid circulation rate at a given vertical aeration rate (vertical aeration rate=4U_{mf}; L_h/D_d= 2.5).

affect the variation of solids circulation rate. From visual observation, adequate bottom aeration reduces the stagnant zone of solid particles as observed in an L-valve [Yang and Knowlton, 1993] and air bypassing occurs at higher aeration rates. Therefore, the optimum bottom aeration rate is 1.5U_{mf} to keep the optimum solids flow rate with good fluidity in the loop-seal.

2-3. Solids Flow Characteristics by Vertical Aeration

Variations of the solid circulation rate and pressure drop in the downcomer (ΔP_d) along the vertical aeration height at a bottom aeration rate of 1.5U_{mf} and a vertical aeration rate of 4.5U_{mf} are shown in Fig. 6. As can be seen, the solid circula-

tion rate and ΔP_d exhibit maximum values along the aeration height irrespective of the variation of gas velocity in the riser. The maximum values are exhibited at the length-to-diameter (L_h/D_d) ratio of 2.5, as found previously that the most effective aeration location is an L_h/D_d ratio of 2 or more above the horizontal section of the L- [Knowlton and Hirsan, 1978] and J-valves [Knowlton et al., 1978]. Based on the pressure balance around the CFB loop (Fig. 3), the pressure drop across the downcomer above the aeration location in a loop-seal is balanced so that ΔP_d must be equal to the sum of the pressure drops through the other elements around the CFB loop. As air is injected at the loop-seal, ΔP_d and the solids circulation rate are a function of aeration rate due to the limited absorbing capacity of the pressure drop across the downcomer [Knowlton and Hirsan, 1978]. This may indicate that higher solids circulation rate can be attained through the loop-seal with longer effective length of downcomer above the aeration point. Therefore, if aeration location is near the bottom of the loop-seal, the effective downcomer length above the aeration location becomes longer so that it can absorb more pressure in the downcomer and consequently increase solids circulation rate. Whereas, if aeration height is too low (below L_h/D_d=2.5), the solid circulation rate becomes lower than that at the higher aeration locations due to gas bypassing or channeling to the riser at the bottom of the loop-seal.

The effect of the vertical aeration rate at aeration location L_h/D_d=2.5 on solid circulation rate and voidage at the upper part of the aeration point in the downcomer is shown in Fig. 7. As can be seen, the solids circulation rate through the loop-seal increases linearly to a maximum value with increasing aeration rates up to 5.5U_{mf} due to the increase of frictional drag on the particles. The voidage at the upper part of the aeration point
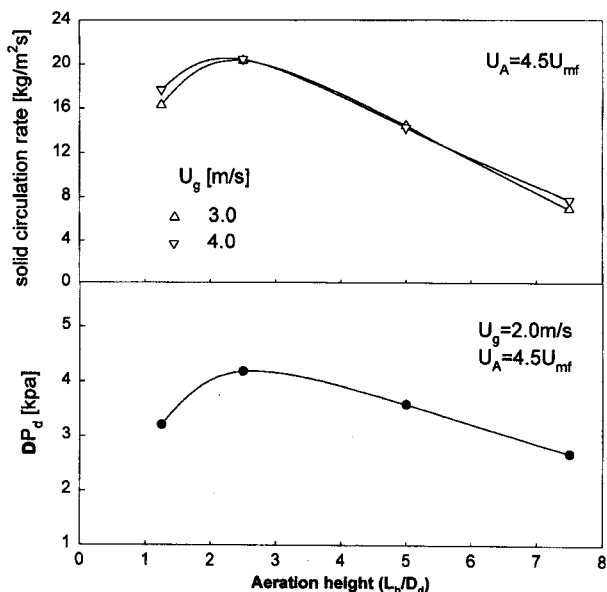

Fig. 6. Effect of vertical aeration height on solid circulation rate and pressure drop in upper downcomer with variation of gas velocity in the riser (I=30 kg).
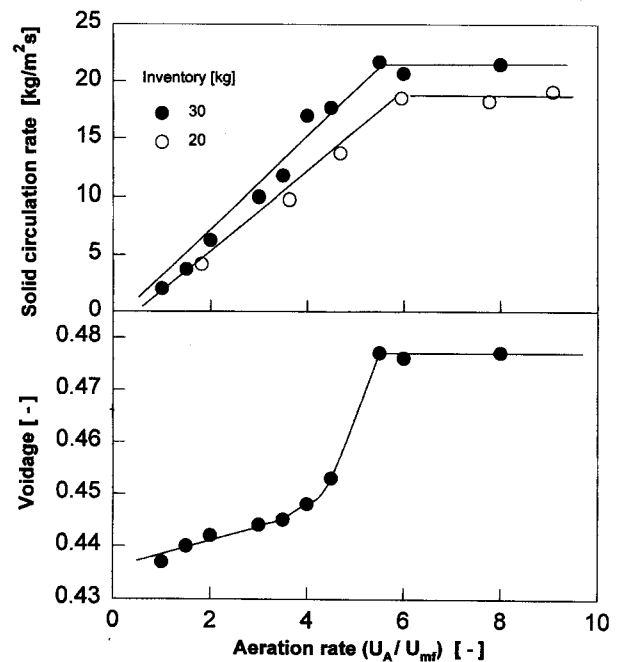

Fig. 7. Effect of vertical aeration velocity on solid circulation rate and voidage in upper downcomer (U_g= 2.0 m/s, I =20, 30 kg, L_h/D_d=2.5).

in the downcomer increases to a constant value with increasing aeration rate. When aerating gas is injected into the loop-seal, the gas flows initially upward through the void between the particles in the downcomer. The relative velocity between gas and solid phases produces frictional drag force on particles in the flow direction so that pressure builds up across the down-comer. When drag force exceeds the force needed to overcome resistance to solids flow, solid particles flow through the valve. The solid flow rate is found to be proportional to the pressure drop across the downcomer. Therefore, as the aeration rate is increased, pressure drop and voidage in the downcomer increase by an increase in slip velocity between gas and solid phases and consequent increase in solid circulation rate. Also, the maximum solid circulation rate increases with increasing solids inventory in a CFB due to the increment of total pressure drop in the downcomer. However, it is observed that larger bubbles or voids stagnate near the aeration point beyond $5.5U_{mf}$. Conceivably, a bubble formed by air injection could have a rising velocity that may be equal to the bulk solid downflow rate [Zenz, 1986]. The stagnant bubble or void obstructs solids downflow since the net opening area to solid flow at that point would be the difference between the cross-sectional areas of the downcomer and a bubble so that solid circulation rate and voidage in the upper downcomer become constant.

2-4. Gas-Solid Flow in the Downcomer

The gas-solid flows in a downcomer are largely divided into non-fluidized, fluidized and streaming flows. The non-fluidized bed flows are divided into packed bed and transitional packed bed flows by slip velocity [Kojabashian, 1958; Zhang and Rudolph, 1991]. Packed bed flow often occurs when the gas flow is assisting solids flow, with the gas pressure higher at the top of the downcomer than at the bottom. Transitional packed bed flow usually occurs when the gas flow is upward relative to the downward solids flow, with the gas pressure at the bottom of the downcomer higher than that at the top, i.e., at the negative pressure gradient condition [Zhang and Rudolph, 1991].

Variation of pressure with height in the downcomer at a given vertical aeration rate is shown in Fig. 8. As can be seen, pressure variation exhibits different tendencies above and below the vicinity of aeration point. Except $U_A=U_{mf}$ with lower solids circulation rates, pressure decreases with the height (increases in direction of solids flow) above the aeration point and increases with the height (decreases in direction of solids flow) below the aeration point. These tendencies can be analyzed by slip velocity, which is the difference between solids velocity (U_s) and actual gas velocity (U_{gd}/ε). The increase in pressure in the direction of solids flow is caused by the positive slip velocity ($U_s > U_{gd}/\varepsilon$) by Eq. (1). Pressure gradient and voidage in the solids flow are less than those at the minimum fluidization condition, and slip velocity is positive. That is typical transitional packed bed flow. However, the pressure decreases in the direction of solids flow below the aeration point since U_{gd}/ε is higher than U_s and slip velocity has negative value in the direction of solids flow [Kojabashian, 1958]. This flow is classified as packed bed flow by Kojabashian's classification [1958]. Variations of pressure gradient and the flow mode near the aeration point are caused by the downflow of injected air. The injected air is put together with air entrained by
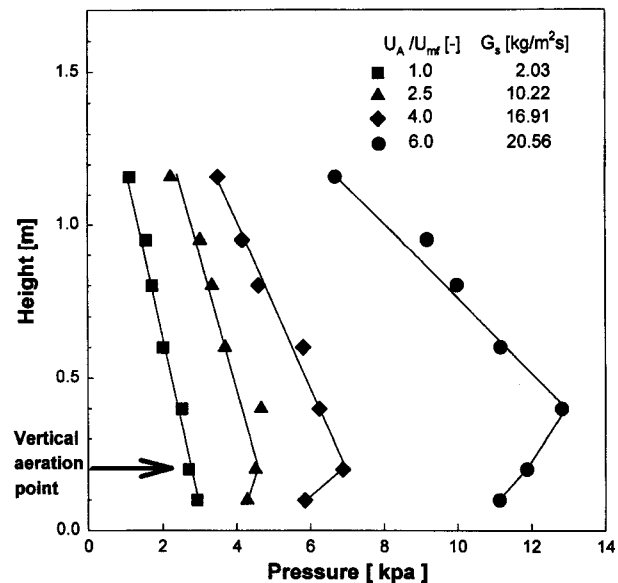
Fig. 8. Variation of pressure with height at different aeration rate in the downcomer [aeration height $(L_h/D_d)=2.5$; I= 30 kg].

solid particles from the upper part of the downcomer so that U_{gd}/ε becomes higher than U_s below the aeration point. However, when aeration rate is low ($U_A=U_{mf}$), U_{gd}/ε is lower than U_s though injected air is added to entrained air below the aeration point. Therefore, the transitional packed bed flow mode continues below the aeration point due to negative slip velocity. Also, when aeration rate is high ($U_A=6U_{mf}$), variation of flow mode occurs at a higher region than the aeration point. Since stagnated large bubbles or voids are formed at a higher region than the aeration point due to high aeration rate, the flow mode changes into packed bed flow near the formed large bubbles or voids.
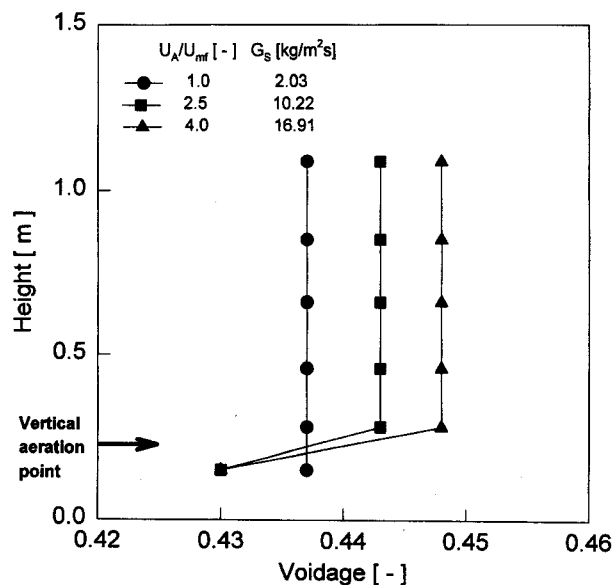

Fig. 9. Variation of voidage with height at different aeration rate in the downcomer [aeration height $(L_h/D_d)=2.5$; I= 30 kg].
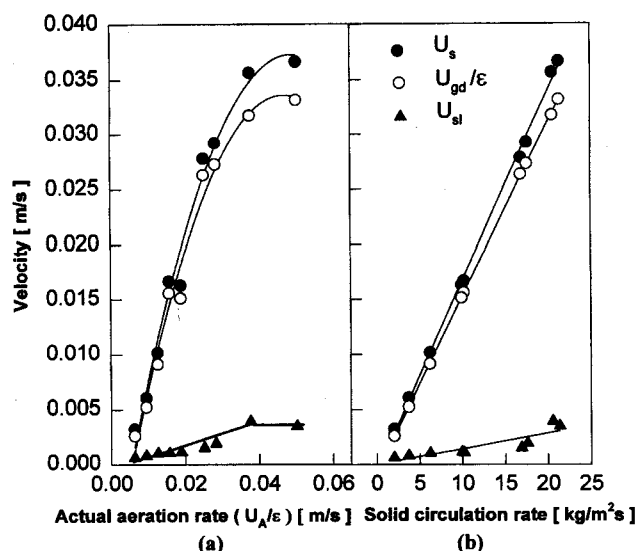
Fig. 10. (a) Effect of actual aeration rate on gas and particle velocities at upper part above aeration point in the downcomer. (b) Effect of solid circulation rate on gas and particle velocities at upper part above the aeration point in the downcomer.

The variation of voidage along the downcomer height at a given vertical aeration rate is shown in Fig. 9. As solid particles flow by aeration, pressure gradient and voidage become constant. As can be seen, the bed voidage shows different trends above and below the aeration point. In the region of transitional packed bed flow above the aeration point, voidage increases with an increment in aeration rate due to the increase of slip velocity. The bed voidage (ε_p) in packed bed flow below the aeration point is 0.43 due to negative slip velocity. However, when the aeration rate is low ($U_A=1.0U_{mf}$), voidage below the aeration point is almost same with that above the aeration point because transitional packed bed flow continues below the aeration point.

The effects of aeration rate and solid circulation rate on U_s, U_g/ε and slip velocity above the aeration point in the downcomer are shown in Fig. 10 in which the positive sign indicates the direction of solid flow in the downcomer. As can be seen, U_s, U_g/ε and slip velocity increase simultaneously since pressure drop and voidage increase with increasing aeration rate and solid circulation rate and consequent increase in slip velocity. In the given experimental ranges, slip velocity and U_g/ε are positive so that gas and solids flow in the same direction [Geldart and Jones, 1991]. The downward gas flow is caused by solids flow downward in the downcomer. In the case of Geldart A particles including FCC particles, a considerable amount of air is retained in their interstices, and air is entrained and descends with solid particles [Dries, 1980; Knowlton, 1988]. The injected air in the loop-seal flows initially upward through voidage between particles so that it builds up pressure in the downcomer. However, as solid particles flow downward at steady state, air goes not upward but downward with solids flow [Geldart and Jones, 1991]. From Figs. 10 (a) and (b), the gas-solid flow in the downcomer can be analyzed as follows: The injected air in the loop-seal flows initially upward in the

downcomer so that it builds up pressure for solids flow. When solid particles flow, the values of U_g/ε and U_s in the upper part of the downcomer are positive (Fig. 10a). It may indicate that solids flow in the downcomer with air that is carried by particles collected by cyclones [Knowlton, 1988; Geldart and Jones, 1991]. The quantity of air carried by solid particles is proportional to the solid circulation rate and air flows through a constant voidage whose value corresponds to pressure gradient in the downcomer with the difference between slip velocity and U_s.

3. Correlation of Solids Circulation Rate

When a mechanical valve is used in the CFB, solids circulation rate is varied with the variation of valve opening. Therefore, the valve equation relates solids flow rate and gas flow rate through an orifice with the pressure drop across an orifice or valve as follows [Rudolph et al., 1991].

$$G_s = C_D \left(\frac{A_o}{A} \right) \sqrt{2\rho_s(1-\varepsilon_{mf})\Delta P_v} \qquad (7)$$

Eq. (7) can be successfully applied to the non-mechanical valve since solids flow mode is almost the same [Yang and Knowlton, 1993]. However, in a non-mechanical valve, the valve opening (A/A_o) in Eq. (7) is not known and is dependent upon the aeration rate. Yang and Knowlton [1993] proposed a correlation to predict solid circulation rate through an L-valve, which relates the valve-opening ratio for injected air quantity, valve size and particle property. However, their correlation cannot be applied to the loop-seal since it has different geometry and aeration configuration. Therefore, assuming the loop-seal as a pneumatically operated pseudo-mechanical valve, the discharge coefficient (C_D) and opening ratio (A/A_o) of the loop-seal are correlated with the dimensionless variables in the present study to predict solids circulation rate from Eq. (7) as:

$$C_D \left(\frac{A_o}{A} \right) = 0.130 \left(\frac{U_{BA}}{U_{mf}} \right)^{0.200} \left(\frac{U_A}{U_{mf}} \right)^{0.372} \left(\frac{L_h}{D_d} \right)^{-0.458} \left(\frac{U_g}{U_t} \right)^{-1.102} \qquad (8)$$

with a correlation coefficient of 0.90 and a standard error of estimate of 7.4×10^{-6}. Therefore, solid circulation rate can be predicted from pressure drop across the loop-seal by Eqs. (7) and (8).

CONCLUSIONS

1. At a constant gas velocity and solid circulation rate, pressure drops across the downcomer and loop-seal increase linearly, but pressure drop across the riser stays almost constant with increasing solids inventory in the downcomer. At a constant solid inventory, pressure drops across the riser and the downcomer increase with increasing solid circulation rate and decreasing gas velocity in the riser.

2. The solid flow rate through the loop-seal increases linearly with increasing aeration rate, whereas it exhibits an ultimate constant value beyond a certain aeration rate.

3. With the same aeration rate at a different aeration location, a maximum solid flow rate attains a height-to-diameter ratio of 2.5 from the horizontal section of the loop-seal. The maximum solid flow rate increases with increasing solid in-

S. W. Kim et al.

ventory in the CFB.

4. Gas-solid flow in the downcomer exhibits different mode such as the transitional packed bed flow and packed bed flow above and below the vicinity of aeration point.

5. As the aeration rate increases, pressure drop and voidage increase above the aeration point in the loop-seal.

6. The obtained solid flow rates have been correlated with pressure drop across the loop-seal with an assumption of a pneumatically operated pseudo-mechanical valve for loop-seal.

NOMENCLATURE

A_v/A : opening ratio of valve [-]
C_D : discharge coefficient [-]
d_p : mean diameter of particle [m]
D_d : diameter of downcomer [m]
G_s : solid circulation rate [kg/m^{2}s]
I : inventory of solid in system [kg]
K : constant [-]
L_h : height of aeration [m]
P : pressure [pa]
ΔP_d : pressure drop across downcomer ($P_{DB} - P_{DT}$ in Fig. 1) [pa]
ΔP_{ls} : pressure drop across loop-seal ($P_{DB} - P_{RB}$ in Fig. 1) [pa]
ΔP_r : pressure drop across riser ($P_{RB} - P_{RT}$ in Fig. 1) [pa]
ΔP_c : pressure drop across cyclone ($P_{RT} - P_{DT}$ in Fig. 1) [pa]
ΔP_v : pressure drop across valve [pa]
U_A : aeration rate [m/s]
U_{BA} : aeration rate at bottom of loop-seal [m/s]
U_g : gas velocity in riser [m/s]
U_{gd} : gas velocity in downcomer [m/s]
U_g/ε : actual gas velocity [m/s]
U_{mf} : minimum fluidization velocity [m/s]
U_s : solid velocity [m/s]
U_{sl} : slip velocity [m/s]
ε : voidage [-]
ε_{mf} : voidage at minimum fluidization condition [-]
ε_p : voidage in packed bed [-]
μ : air viscosity [kg/m s]
ρ_s : apparent density of particle [kg/m^3]
ϕ_s : shape factor [-]

REFERENCES

Basu, P. and Fraser, S. A., "Circulating Fluidized Bed Boiler: Design and Operation", Butterworth-Heinemann, Boston (1991).

Cho, Y. J., Namkung, W., Kim S. D. and Park, S. W., "Effect of Secondary Air Injection on Axial Solid Holdup Distribution in a Circulating Fluidized Bed", J. Chem. Eng. Japan, 27(2), 158 (1994).

Dries, H. W. A., "Cocurrent Gas/Solids Downflow in Vertical Cat Cracker Standpipes: Effects of Gas Compression and Solids Compaction", Fluidization, Editors Grace, J. R. and Matsen, J. M., 493 (1980).

Ergun, S., "Fluid Flow Through Packed Columns", Chem. Eng. Prog., 48(2), 89 (1952).

Knowlton, T. M. and Hirsan, I., "L-valves Characterized for Solids Flow", Hydrocarbon Processing, 57, 149 (1978).

Knowlton, T. M. and Hirsan, I. and Leung, L. S., "The Effect of Aeration Tap Location on the Performance of a J-valve", Fluidization, Editors Davidson, J. F. and Keairns, D. L., Cambridge University Press, 128 (1978).

Knowlton, T. M., "Non Mechanical Solid Feed and Recycle Devices for Circulating Fluidized Bed", CFB Technol. II, Editors Basu, P. and Large, J. F., Pergamon Press, New York, 31 (1988).

Kojabashian, C., "Properties of Dense-phase Fluidized Solids in Vertical Down-flow", Ph.D. Thesis, Massachusetts Institute of Technology, Cambridge, Massachusetts, U.S.A. (1958).

Leung, L. S., Chong, Y. O. and Lottes, J., "Operation of V-valves for Gas-Solid Flow", Powder Technol., 49, 271 (1987).

Merrow, E., "Linking R & D to Problems Experienced in Solids Processing", Chem. Eng. Process., May, 14 (1985).

Namkung, W., Cho, Y. J. and Kim, S. D., "Axial Solid Holdup Distribution in a Circulating Fluidized Bed", HWAHAK KONGHAK, 32, 241 (1994).

Rhodes, M. J. and Laussman, P., "A Study of the Pressure Balance Around the Loop of a CFB", Can. J. Chem. Eng., 70, 625 (1992).

Rudolph, V., Chong, Y. O. and Nicklin, D. J., "Standpipe Modeling for Circulating Fluidized Beds", CFB Technol. III, Editors Basu, P., Horio, M. and Hasatani, M., Pergamon Press, New York, 49 (1991).

Yang, W. C. and Knowlton, T. M., "L-valve Equations", Powder Technol., 77, 49 (1993).

Zenz, F. A., "Maintaining Dense-Phase Standpipe Downflow", Powder Technol., 47, 105 (1986).

Zhang, J. Y. and Rudolph, V., "Transitional Packed Bed Flow in Standpipes", Can. J. of Chem. Eng., 69, 1242 (1991).